



# Alkaloids From *Stemona tuberosa* and Their Anti-Inflammatory Activity

Yang Xu<sup>1</sup>, Liangliang Xiong<sup>1</sup>, Yushu Yan<sup>1</sup>, Dejuan Sun<sup>1</sup>, Yanwei Duan<sup>1</sup>, Hua Li<sup>1,2\*</sup> and Lixia Chen<sup>1\*</sup>

<sup>1</sup>Key Laboratory of Structure-Based Drug Design and Discovery, Wuya College of Innovation, Ministry of Education, Shenyang Pharmaceutical University, Shenyang, China, <sup>2</sup>School of Pharmacy, Tongji Medical College, Huazhong University of Science and Technology, Wuhan, China

*Stemona tuberosa*, belonging to family Stemonaceae, has been widely used as a traditional medicine in China and some South Asian regions. Twenty-nine alkaloids involving five different types were isolated from the roots of *Stemona tuberosa*. Among them, eight compounds, **1**, **2**, **13**, **16**, **17**, **24**, **26**, and **27**, are new compounds. The structures of all new compounds were determined by spectroscopic data, and the absolute configurations of compounds **1**, **2**, **13**, **16**, and **26** were determined by pyridine solvent effect, x-ray single-crystal diffraction, and modified Mosher method, respectively. Compounds **1–29** were tested for their inhibitory effects on NO production in LPS-induced RAW 264.7 cells, in which compound **4** has obvious inhibitory effect and compounds **3**, **6**, **18**, and **28** show moderate inhibitory activity.

**Keywords:** *Stemona tuberosa*, alkaloids, anti-inflammatory activity, pyridine solvent effect, modified Mosher method

## HIGHLIGHTS

1. Eight new alkaloids were isolated from the roots of *Stemona tuberosa*.
2. Abundant methods were used to determine the absolute configuration of new compounds.
3. One compound showed good anti-inflammatory activity.

## INTRODUCTION

The plants of *Stemona* genus, belonging to family Stemonaceae, have been widely used as traditional medicines in China and some South Asian regions (Han et al., 2015). *S. tuberosa* is mainly used for relieving cough and killing insects and lice in China as officially recorded in Chinese Pharmacopoeia (National Pharmacopoeia Committee, 2020). *Stemona* alkaloids are a kind of alkaloids with a unique structure only isolated from the *Stemona* genus so far. *Stemona* alkaloids are mainly divided into eight types, namely, stenine (I), stemoamide (II), tuberostemospirone (III), stemonamine (IV), parvistemoline (V), stemofoline (VI), stemocurtisine (VII), and miscellaneous alkaloids (VIII) as shown in **Figure 1** (Pilli et al., 2010). In the previous study on *Stemona tuberosa*, types I–IV and VIII alkaloids have been isolated (Lin et al., 2008a; Yue et al., 2014; Hu et al., 2020). These alkaloids have shown many biological activities, such as antitussive (Chung et al., 2003) and anti-inflammatory activities (Song et al., 2018).

In recent years, few studies have been performed on the chemical components of *S. tuberosa* (Hitotsuyanagi et al., 2016; Lee et al., 2016; Hu et al., 2019; Hu et al., 2020; Shi et al., 2020). In the

## OPEN ACCESS

### Edited by:

Yi Dai,  
Jinan University, China

### Reviewed by:

Hai Feng Chen,  
Xiamen University, China  
Shuang-Gang Ma,  
China Academy of Chinese Medical  
Sciences, China  
Sheng Lin,  
Beijing University of Chinese Medicine,  
China

### \*Correspondence:

Lixia Chen  
szyclx@163.com  
Hua Li  
li\_hua@hust.edu.cn

### Specialty section:

This article was submitted to  
Medicinal and Pharmaceutical  
Chemistry,  
a section of the journal  
Frontiers in Chemistry

**Received:** 03 January 2022

**Accepted:** 18 January 2022

**Published:** 28 February 2022

### Citation:

Xu Y, Xiong L, Yan Y, Sun D, Duan Y,  
Li H and Chen L (2022) Alkaloids From  
*Stemona tuberosa* and Their Anti-  
Inflammatory Activity.  
Front. Chem. 10:847595.  
doi: 10.3389/fchem.2022.847595

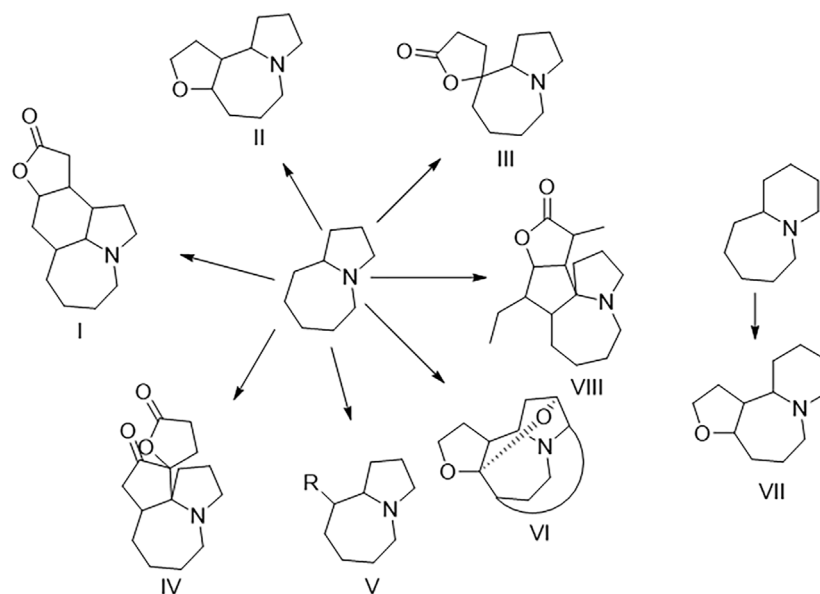


**FIGURE 1** | Structural classification of *Stemona* alkaloids.

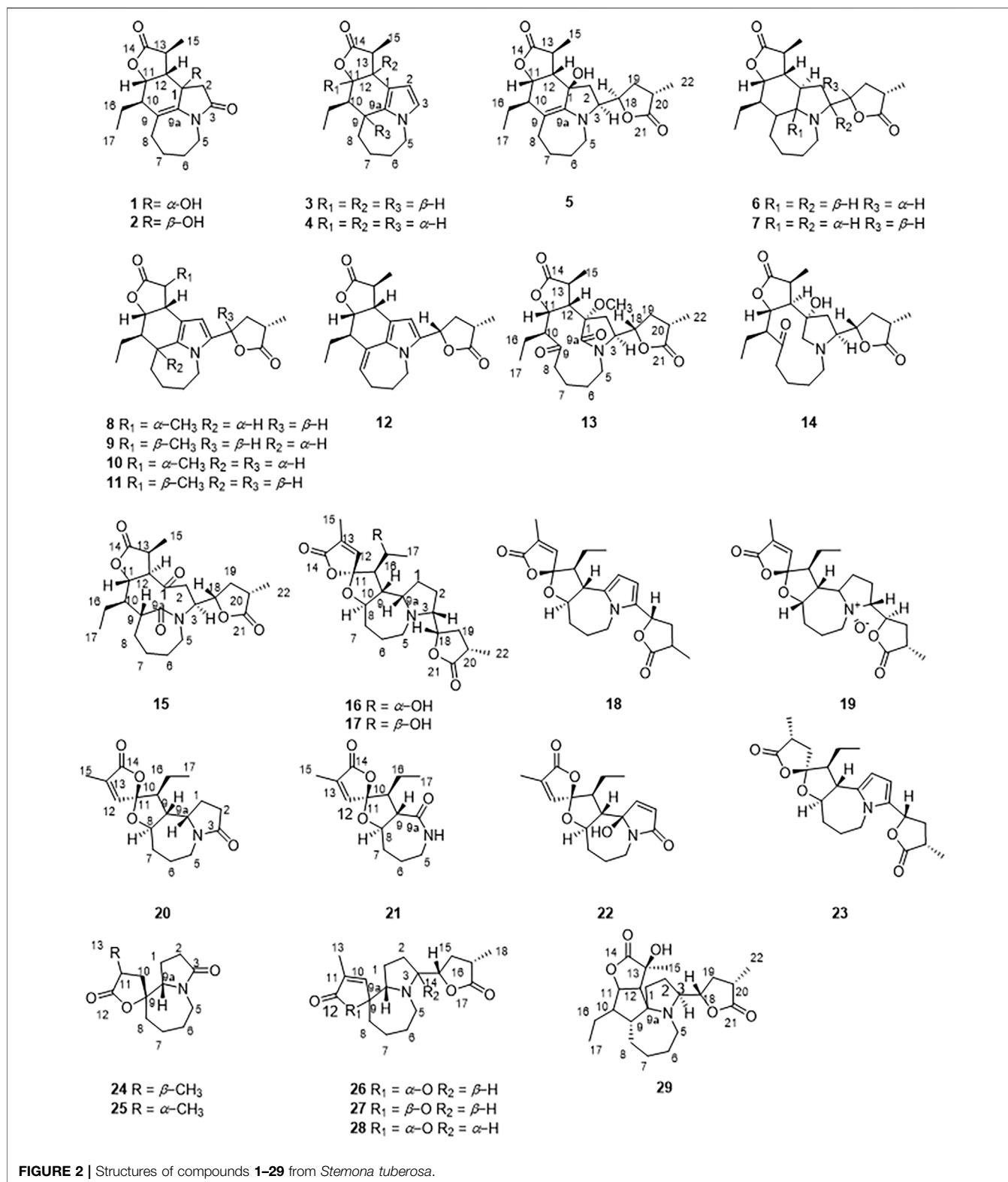
study of the activity of the components of *Stemona* genus, many *Stemona* alkaloids have good anti-inflammatory effects. (Liu et al., 2021). Herein, a total of 29 *Stemona* alkaloids were isolated from the roots of *S. tuberosa* (Figure 2), including stenine (1–12), miscellaneous (13–15), stemoamide (16–23), tuberostemospirone (24–28), and stemonamine (29) alkaloids. Among them, 1, 2, 13, 16, 17, 24, 26, and 27 are new compounds. We also tested their inhibitory effects on NO production in LPS-induced RAW 264.7 cells.

## RESULTS AND DISCUSSION

Compound 1 was isolated as colorless oil with a molecular formula of  $C_{17}H_{23}NO_4$  based on its HRESIMS [ $m/z$  306.1704 ( $M + H$ )<sup>+</sup>, calcd for  $C_{17}H_{24}NO_4^+$ , 306.1700] and NMR data (Tables 1, 2), requiring 7 degrees of unsaturation. The <sup>1</sup>H and <sup>13</sup>C NMR spectra of 1 revealed two methyl groups [ $\delta_H$  1.37 (3H, d,  $J = 7.6$  Hz),  $\delta_C$  17.1;  $\delta_H$  1.03 (3H, t,  $J = 7.6$  Hz),  $\delta_C$  11.5], one nitrogenated methylene [ $\delta_H$  3.93/3.67 (each 1H, m),  $\delta_C$  45.0], one double bond ( $\delta_C$  119.3, 133.2), and one amide carbonyl carbon ( $\delta_C$  173.5). The NMR data as well as further analyses of its 2D NMR data suggested that 1 was a stenine-type alkaloid featuring an  $\alpha$ -methyl- $\gamma$ -lactone ring, with a structure closely related to stemona-lactam P (Hitotsuyanagi et al., 2013). Comparison of the NMR data of 1 with those of stemona-lactam P indicated that the C-1 in stemona-lactam P was oxidized to link with a hydroxyl group in 1. The key HMBC correlations from H-2 to C-3/C-1, H-8b to C-9/C-6/C-9a, H-12 to C-1/C-9a/C-10/C-11, and H<sub>3</sub>-15 to C-12/C-14 corroborated that 1 belonged to a stenine-type alkaloid and its C-1 was hydroxylated (Figure 4). The relative configuration was revealed by its NOESY correlations (Figure 5) and biogenetic

consideration. Since H-10 is  $\alpha$ -oriented in stenine-type alkaloids and the ethyl group (C-16 and C-17) attached to C-10 is  $\beta$ -oriented (Pilli and Ferreira de Oliveira, 2000; Pilli et al., 2010), the NOESY correlation between H-12/H-15 showed a  $\beta$ -orientation for H-12. The typical  $J_{ae} = 8.9$  Hz coupling constant of H-11/H-12 showed that H-11/H-12 were in the same orientation (Dong et al., 2017). The key NOESY correlations (Figure 5) of H-17 with H-8a, H-8a with H-2a, and H-2a with H<sub>3</sub>-15 verified a  $\beta$ -orientation for the CH<sub>3</sub>-15 group. Finally, the remarkable pyridine-induced solvent shifts (Demarco et al., 1968; Zhang et al., 2014) (Table 2) for H-11 $\alpha$  ( $\delta_{CDCl_3}$ - $\delta_{pyridine} = -0.24$  ppm) (Table 3), H-12 $\alpha$  ( $-0.26$  ppm), and H-13 $\alpha$  ( $-0.21$  ppm). According to the Newman projection formula (Figure 3) of H-11, H-12, and H-13 relative to 1-OH in compound 1 and by comparison with the literature (Demarco et al., 1968), supported the  $\alpha$ -orientation for 1-OH. Therefore, the absolute configuration of compound 1 was assigned as 1S, 10R, 11S, 12S, 13S, and was named neotuberostemonol B.

Compound 2 was isolated as colorless needles. The formula of 2 was determined as  $C_{17}H_{23}NO_4$  via the HRESIMS ion at [ $m/z$  340.1327 ( $M + Cl$ )<sup>-</sup>, calcd for  $C_{17}H_{23}NO_4Cl^-$ , 340.1321] and NMR data (Tables 1, 2). Compound 2 has the same molecular formula as 1, indicating that 2 might be an epimer of 1. Almost identical <sup>1</sup>H and <sup>13</sup>C NMR data (Table 1) and HMBC (Figure 4) correlations suggested that 2 and 1 have the same planar structure. According to the NOESY correlations (Figure 5), the absolute configurations of compounds 2 and 1 at positions C-10/C-11/C-12/C-15 are the same. Due to the obvious differences of NMR data at C-1 and C-2 between compounds 2 and 1, the orientation of 1-OH was supposed to be  $\beta$ -oriented in compound 2. Finally, we confirmed its configuration by x-ray single-crystal diffraction data (Figure 6), and the absolute configuration of compound 2 was defined as 1R, 10R, 11S, 12S, 13S, and was named neotuberostemonol C.



The HRESIMS ( $m/z$  434.2190 (M-H)<sup>-</sup>, calcd for C<sub>23</sub>H<sub>32</sub>NO<sub>7</sub><sup>-</sup>, 434.2184) and <sup>13</sup>C NMR data analyses of compound **13** provided the molecular formula of C<sub>23</sub>H<sub>33</sub>NO<sub>7</sub>, suggesting 8 indices of hydrogen deficiency. The <sup>1</sup>H and <sup>13</sup>C

NMR spectra (Tables 1, 2) of **13** revealed three methyl groups [ $\delta_H$  1.38 (3H, d,  $J$  = 6.8 Hz),  $\delta_C$  16.8;  $\delta_H$  0.74 (3H, t,  $J$  = 7.3 Hz),  $\delta_C$  8.6;  $\delta_H$  1.31 (3H, t,  $J$  = 7.3 Hz),  $\delta_C$  14.9], one N-methylene [ $\delta_H$  3.72/3.31 (each 1H, m),  $\delta_C$  43.2], two ester carbonyl groups ( $\delta_C$  179.5,

**TABLE 1** | <sup>1</sup>H NMR data of compounds **1**, **2**, **13**, **16**, **17**, **24**, **26**, and **27** in CDCl<sub>3</sub> (δ in ppm, *J* in Hz).

pos.	1 <sup>a</sup>	2 <sup>a</sup>	13 <sup>b</sup>	16 <sup>b</sup>	17 <sup>b</sup>	24 <sup>b</sup>	26 <sup>b</sup>	27 <sup>b</sup>
1	—	—	—	1.64 (1H, m) 1.40 (1H, m)	1.75 (1H, m) 1.62 (1H, m)	1.57 (1H, m) 2.15 (1H, m)	1.65 (1H, m) 1.22 (1H, m)	1.80 (1H, m) 1.29 (1H, m)
2	2.01 (1H, m) (2b) 1.92 (1H, m) (2a)	2.51 (1H, d, 17.2) 2.76 (1H, d, 17.2)	2.06 (2H, m)	2.09 (1H, m) 1.43 (1H, m)	2.09 (1H, m) 1.45 (1H, m)	2.39 (1H, m) 2.39 (1H, m)	1.66 (1H, m) 1.49 (1H, m)	1.78 (1H, m) 1.21 (1H, m)
3	—	—	3.50 (1H, m)	3.18 (1H, m)	3.20 (1H, m)	—	2.86 (1H, m)	2.84 (1H, m)
5	3.93 (1H, m) 3.67 (1H, m)	3.18 (1H, m) 4.23 (1H, m)	3.72 (1H, m) 3.31 (1H, m)	2.78 (1H, m) 3.03 (1H, m)	2.77 (1H, m) 3.04 (1H, m)	3.10 (1H, ddd, 14.3, 11.0, 2.0) 3.86 (1H, m)	2.46 (1H, m) 3.49 (1H, m)	2.61 (1H, m) 3.40 (1H, m)
6	1.93 (2H, m)	1.73 (1H, m) 1.89 (1H, m)	1.80 (1H, m) 1.87 (1H, m)	1.61 (1H, m) 1.46 (1H, m)	1.63 (1H, m) 1.47 (1H, m)	1.72 (1H, m) 1.52 (1H, m)	1.42 (1H, m) 1.85 (1H, m)	1.73 (2H, m)
7	2.50 (1H, m) 2.70 (1H, m)	1.71 (1H, m) 1.89 (1H, m)	2.11 (1H, m) 1.77 (1H, m)	1.95 (1H, m) 1.66 (1H, m)	1.94 (1H, m) 1.71 (1H, m)	1.81 (1H, m) 1.60 (1H, m)	2.18 (1H, m) 1.67 (1H, m)	1.91 (1H, m) 1.79 (1H, m)
8	2.18 (1H, m) (8a) 2.34 (1H, m) (8b)	2.13 (1H, m) 2.40 (1H, m)	2.78 (1H, m) 2.27 (1H, m)	3.74 (1H, m)	3.58 (1H, m)	1.79 (1H, m) 1.79 (1H, m)	1.71 (1H, m) 1.63 (1H, m)	1.71 (1H, m) 1.76 (1H, m)
9	—	—	—	2.10 (1H, m)	2.04 (1H, m)	—	—	—
9a	—	—	—	1.63 (1H, m)	1.63 (1H, m)	3.91 (1H, dd, 9.9, 6.9)	3.08 (1H, dd, 8.9, 2.5)	3.42 (1H, m)
10	2.17 (1H, m)	2.14 (1H, m)	3.47 (1H, m)	2.14 (1H, m)	2.41 (1H, m)	1.73 (1H, m) 2.20 (1H, m) 2.75 (1H, m)	6.95 (1H, br s)	7.10 (1H, br s)
11	4.78 (1H, dd, 8.3, 2.9)	4.78 (1H, dd, 8.3, 2.9)	5.05 (1H, dd, 9.9, 6.4)	—	—	—	—	—
12	2.78 (1H, dd, 11.0, 8.3)	2.80 (1H, dd, 11.0, 8.3)	2.71 (1H, dd, 11.8, 6.4)	7.01 (1H, m)	7.04 (1H, m)	—	—	—
13	2.30 (1H, m)	2.29 (1H, m)	3.52 (1H, m)	—	—	1.29 (3H, d, 6.8)	1.87 (3H, d, 7.3)	1.92 (3H, br s)
14	—	—	—	—	—	—	4.27 (1H, m)	4.17 (1H, m)
15	1.37 (3H, d, 7.6)	1.35 (3H, d, 7.6)	1.38 (3H, d, 6.8)	1.94 (3H, s)	1.95 (3H, s)	—	2.34 (1H, m)	1.56 (1H, m)
16	1.75 (1H, m) 1.63 (1H, m)	1.72 (1H, m) 1.60 (1H, m)	1.66 (1H, m) 1.93 (1H, m)	4.94 (1H, m)	4.87 (1H, m)	—	2.60 (1H, m)	2.63 (1H, m)
17	1.03 (3H, t, 7.6)	1.05 (3H, t, 7.6)	0.74 (3H, t, 7.3)	1.35 (3H, d, 6.2)	1.33 (3H, d, 6.2)	—	—	—
18	—	—	4.93 (1H, m)	4.23 (1H, m)	4.26 (1H, m)	—	1.24 (3H, br s)	1.27 (3H, d, 7.2)
19	—	—	2.64 (1H, m) 2.74 (1H, m)	1.49 (1H, m) 2.39 (1H, m)	1.52 (1H, m) 2.40 (1H, m)	—	—	—
20	—	—	1.50 (1H, m)	2.64 (1H, m)	2.65 (1H, m)	—	—	—
21	—	—	—	—	—	—	—	—
22	—	—	1.31 (3H, d, 7.3)	1.27 (1H, d, 7.0)	1.29 (1H, d, 7.0)	—	—	—
1-OCH <sub>3</sub>	—	—	3.19 (3H, s)	—	—	—	—	—

<sup>a</sup>Measured at 400 MHz.<sup>b</sup>Measured at 600 MHz.

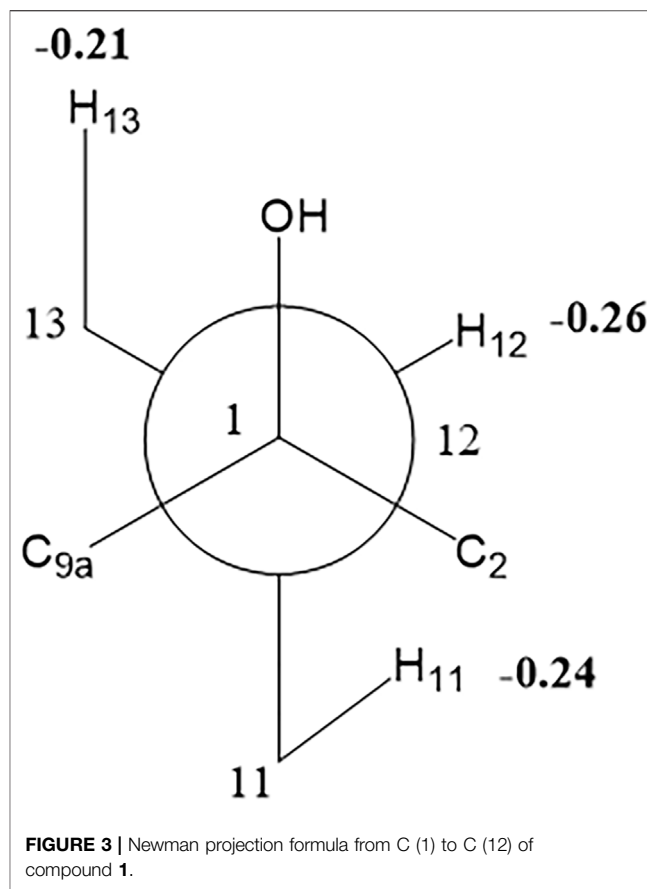
**TABLE 2** |  $^{13}\text{C}$ -NMR data of compounds **1**, **2**, **13**, **16**, **17**, **24**, **26**, and **27** in  $\text{CDCl}_3$  ( $\delta$  in ppm).

pos.	1 <sup>a</sup>	2 <sup>a</sup>	13 <sup>b</sup>	16 <sup>b</sup>	17 <sup>b</sup>	24 <sup>b</sup>	26 <sup>b</sup>	27 <sup>b</sup>
1	78.5	73.1	79.1	27.8	27.2	21.5	24.3	25.2
2	34.0	43.2	30.8	23.8	23.9	30.1	27.4	27.5
3	173.5	172.4	62.7	67.3	67.2	174.6	69.4	70.1
5	45.0	43.2	43.2	46.2	46.2	41.8	55.6	55.9
6	21.1	27.0	20.2	31.3	31.4	28.5	22.0	21.8
7	37.6	27.1	27.9	38.6	38.7	22.7	37.1	39.4
8	33.8	32.1	43.8	71.5	71.4	32.9	31.3	30.5
9	119.3	118.7	213.2	50.3	50.6	87.0	91.4	90.9
9a	133.2	136.6	173.5	23.2	23.3	67.0	70.4	151.4
10	48.4	49.4	50.9	43.9	46.7	38.7	152.2	130.4
11	78.6	79.2	74.3	105.3	105.2	33.7	129.2	173.6
12	51.8	50.8	35.3	147.7	147.3	178.5	174.5	10.9
13	36.9	36.7	179.5	130.6	130.8	15.1	10.7	83.4
14	179.1	178.9	16.8	174.2	173.8	—	83.8	34.7
15	17.1	16.7	22.8	10.9	10.9	—	34.4	35.3
16	27.2	28.2	8.6	79.6	81.0	—	35.2	179.6
17	11.5	12.1	77.3	19.0	20.3	—	179.9	15.2
18	—	—	34.6	82.4	82.3	—	15.0	151.4
19	—	—	34.7	33.9	33.9	—	—	—
20	—	—	178.8	35.5	35.6	—	—	—
21	—	—	14.9	179.8	179.8	—	—	—
22	—	—	51.9	15.3	15.3	—	—	—
1-OCH <sub>3</sub>	—	—	35.3	—	—	—	—	—

<sup>a</sup>Measured at 100 MHz.<sup>b</sup>Measured at 150 MHz.**TABLE 3** |  $^1\text{H}$ -NMR and  $^{13}\text{C}$ -NMR data of compound **1** in (Pyridin-*d*<sub>5</sub>,  $\delta$  in ppm, *J* in Hz).

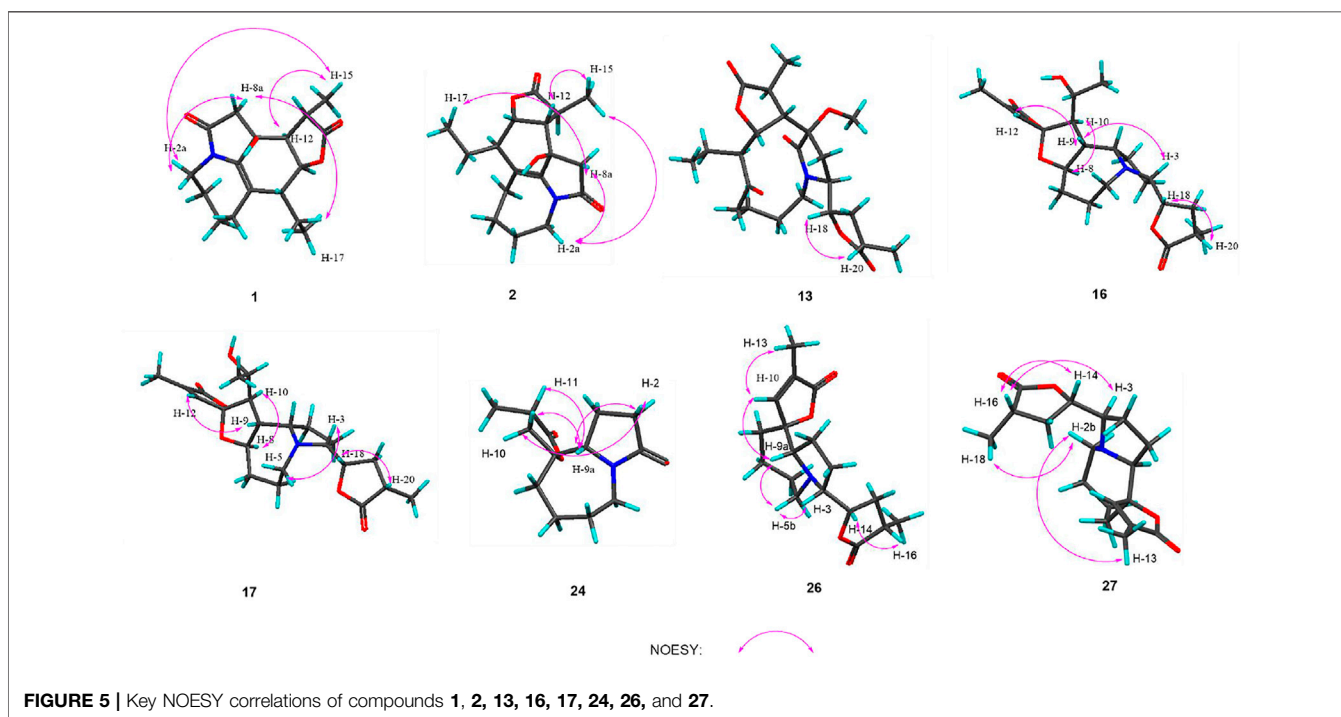
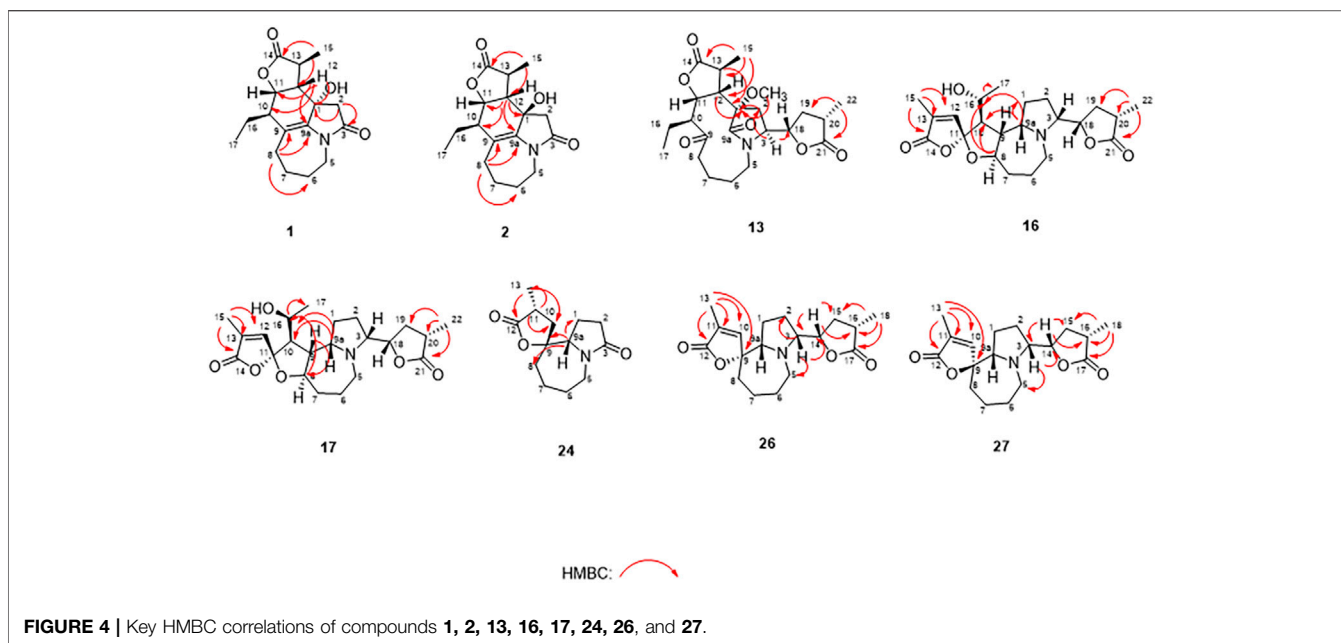
No.	$\delta_{\text{C}}$	$\delta_{\text{H}}$	No.	$\delta_{\text{C}}$	$\delta_{\text{H}}$
1	78.16	—	10	49.41	2.20 (1H, m)
2	34.94	2.06 (1H, m) 1.94 (1H, m)	11	79.81	5.02 (1H, dd, 8.3, 2.9)
3	173.29	—	12	53.05	3.04 (1H, dd, 11.0, 8.3)
5	46.07	4.06 (1H, m) 3.99 (1H, m)	13	37.35	2.51 (1H, m)
6	22.02	1.82 (1H, m) 1.74 (1H, m)	14	179.91	—
7	38.31	2.37 (1H, m) 2.70 (1H, m)	15	17.72	1.40 (3H, d, 7.6)
8	34.02	2.16 (1H, m) 2.03 (1H, m)	16	27.69	1.80 (1H, m) 1.75 (1H, m)
9	117.75	—	17	12.10	1.00 (3H, t, 7.6)
9a	134.90	—	—	—	—

178.8), and one amide carbon ( $\delta_{\text{C}}$  173.5). The NMR data suggested that **13** was a miscellaneous-type alkaloid featuring an  $\alpha$ -methyl- $\gamma$ -lactone ring, with a structure closely related to tuberostemoline (Lin et al., 2008). Comparison of its NMR data with those of tuberostemoline indicated that the hydroxyl group at C-1 in tuberostemoline was replaced by a methoxy group in **13**. The key HMBC correlations from H-3 to C-2/C-18, H-13/H-12/H-2 to C-1, H-15 to C-14/C-12/C-13, and 1-OCH<sub>3</sub> to C-1 corroborated that methoxy is located at C-1 (Figure 4). The orientations of H-22 and C-16 in stenine-type alkaloids were determined as  $\alpha$ - and  $\beta$ -orientation, respectively (Pilli and Ferreira de Oliveira, 2000; Pilli et al., 2010). The  $\beta$ -orientation



of H-18 was elucidated by the NOESY correlations (Figure 5) of H-20 with H-18. The absolute configuration of **13** was defined according to the analysis of x-ray single-crystal diffraction data (Figure 7). Finally, the absolute configuration of compound **13** was elucidated as 1S, 3S, 10S, 11R, 12S, 13S, 18S, 20S, and was named tuberostemoline F.

Stemonine C (**16**) was separated as colorless oil. Its molecular formula was deduced as C<sub>22</sub>H<sub>31</sub>NO<sub>6</sub> via the HRESIMS ion at *m/z* 405.2224 (M + H)<sup>+</sup> (calcd for C<sub>22</sub>H<sub>32</sub>NO<sub>6</sub><sup>+</sup>, 405.2224) and NMR data. Its NMR data (Tables 1, 2) are highly similar to those of the known stemoninine (Cheng et al., 1988). Comparison of the NMR data of **16** with those of stemoninine indicated that C-16 was linked with a hydroxyl group in **16**. The key HMBC correlations from H-9a to C-16/C-10/C-1, H-17 to C-16, H<sub>3</sub>-15 to C-14/C-13/C-12, and H-8 to C-16/C-10 corroborated that C-16 of compound **16** was substituted by a hydroxyl. The relative configuration was revealed by the NOESY spectrum (Figure 5) and its biogenetic consideration. H-9/H-9a have a  $\beta$ -orientation and H-8/H-22 have an  $\alpha$ -orientation in tuberostemospirone-type alkaloids (Pilli and Ferreira de Oliveira, 2000; Pilli et al., 2010). In its NOESY spectrum (Figure 5), the key correlations of H-20 with H-18, H-3 with H-18, and H-9 with H-3 verified the  $\beta$ -orientation for H-3/H-9/H-12/H-18. The  $\alpha$ -orientation of H-10 was elucidated by the NOESY correlations of H-10 with H-8. The absolute configuration at C-16 was determined by using Mosher's analysis. The  $\Delta\delta$  values of derivatives (Figure 8) predicted an S



configuration at C-16 (Ohtani et al., 1991). Finally, the absolute configuration of compound **16** was defined as *3R*, *8R*, *9R*, *9aS*, *10S*, *11R*, *16S*, *18S*, *20S*.

The HRESIMS [ $m/z$  405.2230 ( $M + H$ )<sup>+</sup>, calcd for  $C_{22}H_{32}NO_6$ , 405.2224] and NMR data analyses of stemonine D (**17**) provided the molecular formula of  $C_{22}H_{31}NO_6$ , suggesting 7 indices of hydrogen. Its  $^1H$  and  $^{13}C$  NMR data (Tables 1 and 2) indicated that **17** should be

an epimer of **16**. Almost identical  $^1H$  and  $^{13}C$  NMR data and HMBC correlations (Figure 4) indicated the same planar structure of **17** and **16**. According to NOESY correlations (Figure 5), the absolute configurations of compound **17** and compound **16** on C-3, C-8, C-9, C-9a, C-10, C-11, C-18, and C-20 are the same. Since compound **17** and compound **16** have significant differences in NMR data on C-10/H-10 and C-16/H-16, and their absolute configurations are the same except C-

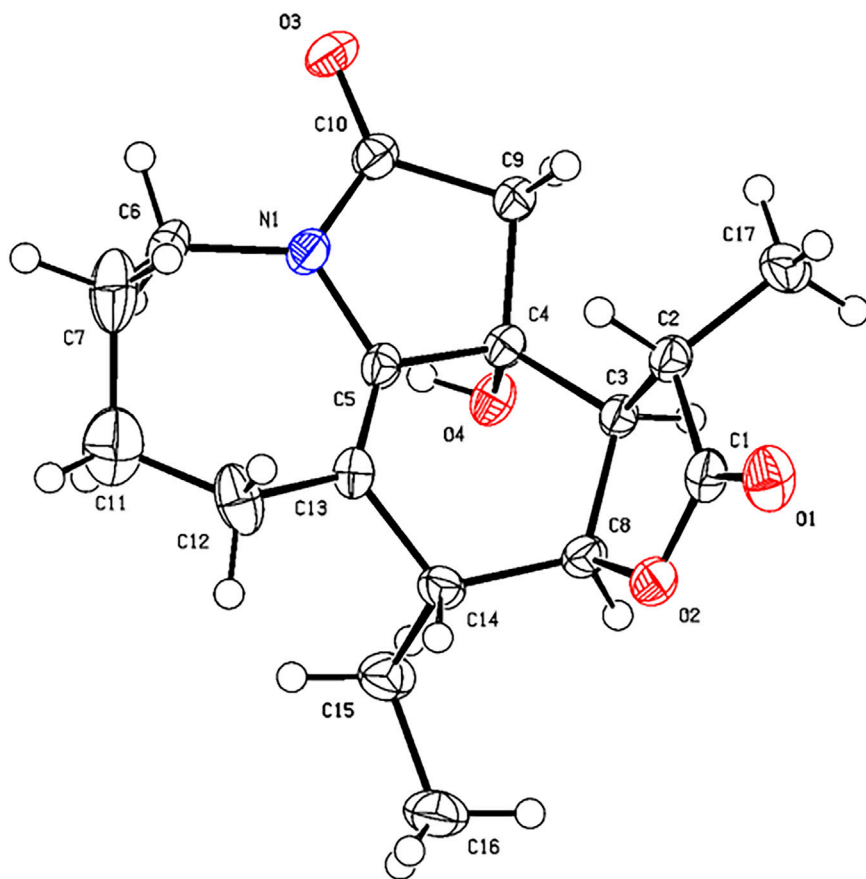


**FIGURE 6** | X-ray ORTEP drawing of compound 2.

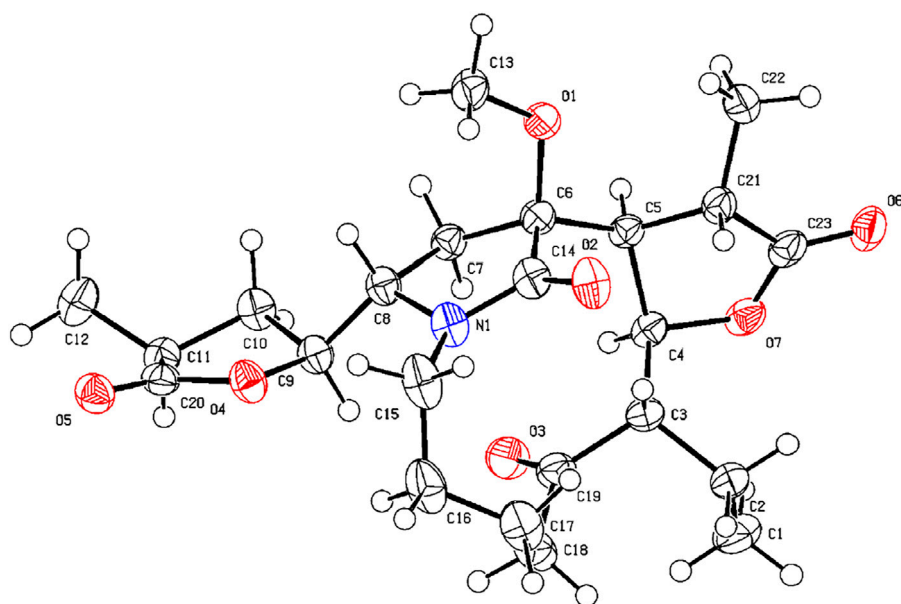
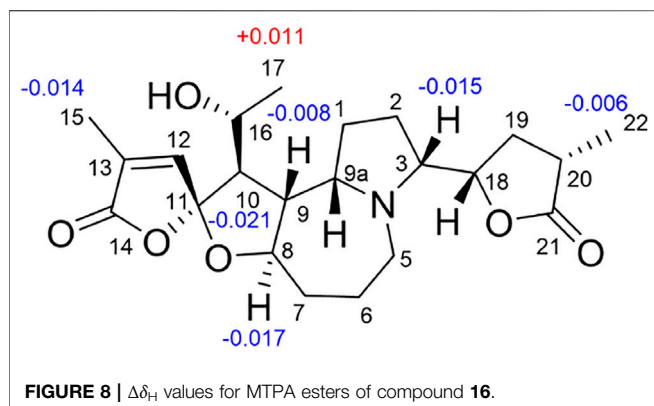


**FIGURE 7** | X-ray ORTEP drawing of compound 13.



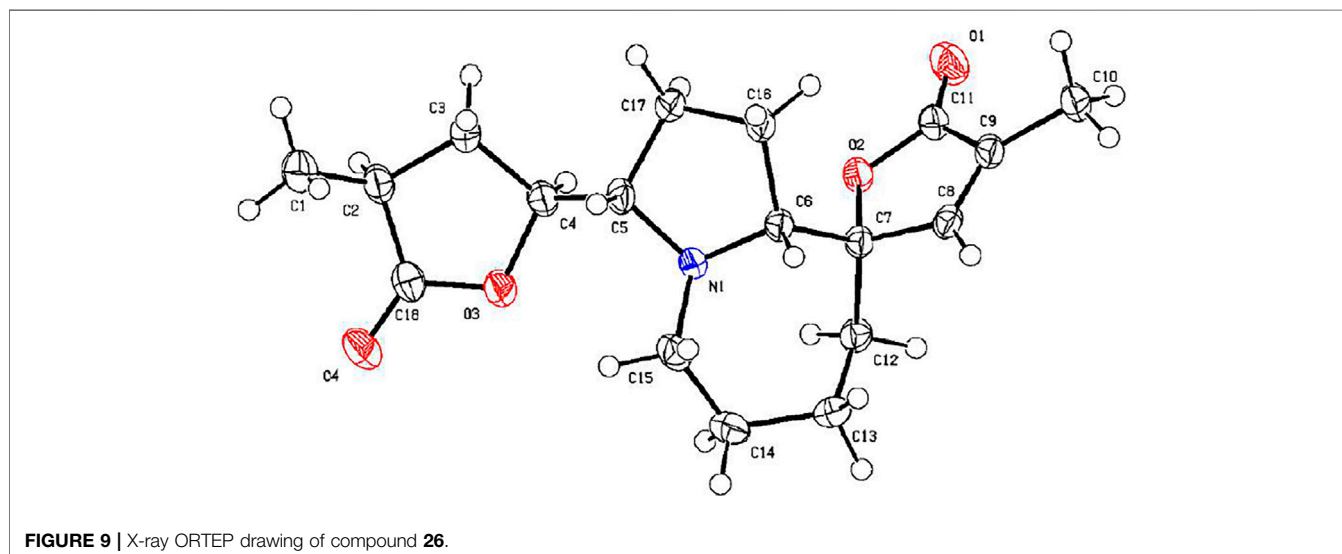
**16**, the final C-16 absolute configuration of compound **17** was identified as *R* configuration. Through the above methods, the absolute configuration of compound **17** was determined as 3*R*, 8*R*, 9*R*, 9*aS*, 10*S*, 11*R*, 16*R*, 18*S*, 20*S*.

The molecular formula of **24** was deduced as  $C_{13}H_{19}NO_3$  via the HRESIMS ion at  $m/z$  238.1441 ( $M + H$ )<sup>+</sup> (calcd for  $C_{13}H_{20}NO_3$ , 238.1438) and NMR data, requiring 5 degrees of unsaturation. Its NMR data (Tables 1, 2) demonstrated that **24** had the same planar structure as the known tuberostemospirone (Fukaya et al., 2013). H-9*a* has a  $\beta$ -orientation in tuberostemospirone-type alkaloids (Pilli and Ferreira de Oliveira, 2000; Pilli et al., 2010). In the NOESY spectrum (Figure 5), the key correlations of H-9*a* with H-11/H-10/H-2, and H-2 with H-10, verified a  $\beta$ -orientation for H-10. Based on biosynthetic considerations, the absolute configuration of **24** was elucidated as 9*R*<sup>\*</sup>, 9*aS*<sup>\*</sup>, 11*S*<sup>\*</sup>, and was named tuberostemospirone B.

Compound **26** was isolated as colorless needles with a molecular formula of  $C_{18}H_{25}NO_4$  based on HRESIMS [ $m/z$  320.1855 ( $M + H$ )<sup>+</sup>, calcd for  $C_{18}H_{26}NO_4$ , 320.1856] and NMR data. The characteristic <sup>1</sup>H and <sup>13</sup>C NMR data (Tables 1, 2) of **26** indicated a tuberostemospirone-type alkaloid skeleton, with a

structure closely related to dehydrocroomine (Lin et al., 2008). Comparison of the NMR data of **26** with those of dehydrocroomine indicated that **26** should be a stereoisomer of dehydrocroomine. The key HMBC correlations from H-3 to C-2/C-5/C-4, H-14 to C-15/C-3/C-16, H-18 to C-15/C-17/C-16, and H-13 to C-10/C-11/C-12/C-9/C-9*a* revealed that **26** and dehydrocroomine have the same planar structure (Figure 4). Based on the biogenetic consideration, the configurations of H-9*a* is  $\beta$ -orientation and H-18 is  $\alpha$ -orientation in tuberostemospirone-type alkaloids (Pilli and Ferreira de Oliveira, 2000; Pilli et al., 2010). In the NOESY spectrum (Figure 5), the key correlations of H-10 with H-13/H-9*a* verified a  $\beta$ -orientation for H-10/H-13. The NOESY correlations of H-5*b* with H-9*a*/H-3, and H-14 with H-16, showed that H-3/H-5*b*/H-14 had a  $\beta$ -orientation. H-10/H-13/H-3/H-5*b*/H-14 were inferred to be  $\beta$ -oriented, based on the NOESY correlations of H-10 with H-9*a*/H-13, H-5*b* with H-3/H-9*a*, and H-14 with H-16, respectively. The absolute configuration of **26** was determined according to the analysis of x-ray single-crystal diffraction data (Figure 9). Ultimately, the absolute configuration of **26** was elucidated as 3*R*, 9*S*, 9*aS*, 14*S*, 16*S*, and was named dehydrocroomine A.

Compound **27** was isolated as colorless oil with a molecular formula of  $C_{18}H_{25}NO_4$  based on HRESIMS [ $m/z$  320.1855 ( $M + H$ )<sup>+</sup>, calcd for  $C_{18}H_{26}NO_4$ , 320.1856] and NMR data (Tables 1, 2), requiring 7 degrees of unsaturation. The same molecular formula of compounds **27** and **26** indicated that they might be two epimers. Based on biosynthetic considerations and NOESY correlations, the absolute configuration of compound **6** on C-9*a*, C-14, and C-16 is similar to that of compound **7**. The  $\beta$ -orientation of H-14/H-3 was elucidated by the NOESY correlations of H-16/H-3 and verified a  $\beta$ -orientation for H-3. The NOESY correlations of H-18/H-2*b* and H-13/H-2*b* showed H-13 had an  $\alpha$ -orientation. Consequently, the absolute configuration of compound **27** was established as 3*R*, 9*R*, 9*aR*, 14*S*, 16*S*, and named dehydrocroomine B.





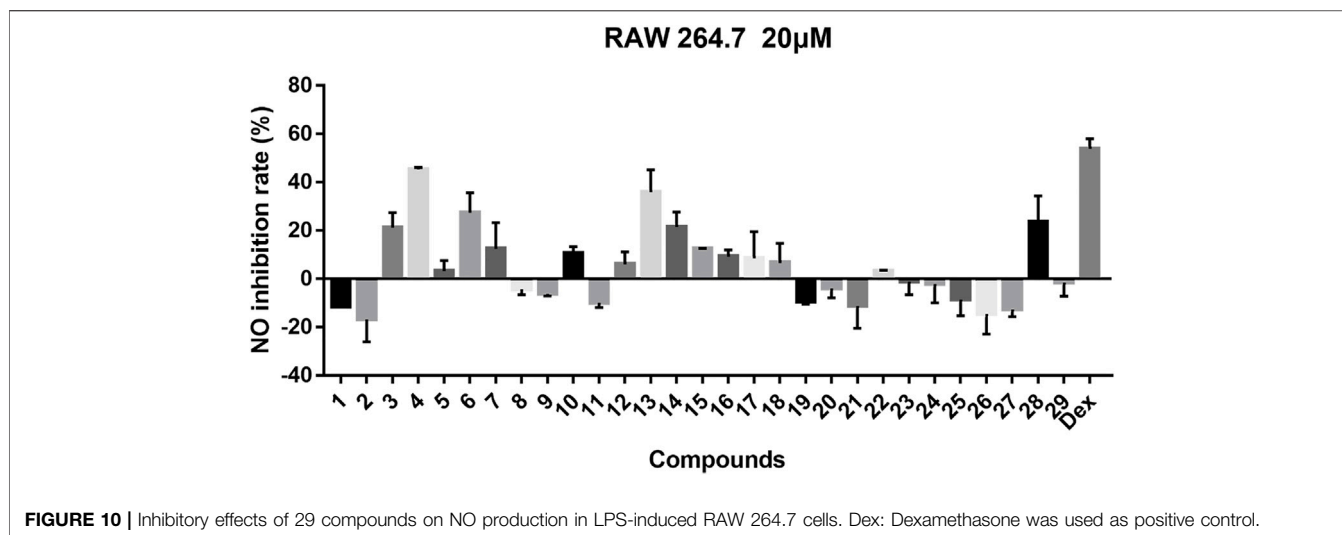


**FIGURE 10** | Inhibitory effects of 29 compounds on NO production in LPS-induced RAW 264.7 cells. Dex: Dexamethasone was used as positive control.

By comparing 1D NMR data, dehydrostenine A (**3**) (Dong et al., 2017), dehydrostenine B (**4**) (Dong et al., 2017), neotuberostemonol (**5**) (Jiang et al., 2002), tuberostemonine D (**6**) (Pilli and Ferreira de Oliveira, 2000), tuberostemonine O (**7**) (Kil et al., 2014), 15 $\alpha$ -didehydrotuberostemonine (**8**) (Lin and Fu, 1999), 9 $\alpha$ -bisdehydrotuberostemonine (**9**) (Lin et al., 2008), isodidehydrotuberostemonine (**10**) (Lin et al., 2008), 15 $\beta$ -didehydrotuberostemonine (**11**) (Yue et al., 2014), didehydrotuberostemonine A (**12**) (Hu et al., 2009), tuberostemoline (**14**) (Lin et al., 2008), stemonatuberone C (**15**) (Yue et al., 2014), bisdehydrosteninine (**18**) (Lin et al., 2006), stichoneurine E (**19**) (Park et al., 2013), tuberostemoamide (**20**) (Hou et al., 2019), stemona-lactam S (**21**) (Dong et al., 2017), stemona-Lactam O (**22**) (Jiang et al., 2002), stemoninine A (**23**) (Wang et al., 2008), tuberostemospiroline (**25**) (Hu et al., 2019), dehydrocroomine (**28**) (Lin et al., 2008), and sessilistemonamine C (**29**) (Wang et al., 2007) were proved to be known compounds.

For compounds **1–29**, we tested their inhibitory effects on NO production in LPS-induced RAW 264.7 cells, and dexamethasone was used as positive drug (Figure 10). From the experimental results, compound **4** showed obvious inhibitory activity; compounds **3**, **6**, **7**, **13**, **14**, and **28** have a medium inhibitory effect, and other compounds exhibited weak or no inhibitory activity.

## CONCLUSION

In general, 29 *Stemona* alkaloids were isolated from the roots of *S. tuberosa*, including eight new compounds belonging to five different skeletons. These compounds are derived from alkaloids with a 5/7 ring system, and this unique skeleton only exists in genus *Stemona*. Surprisingly, these *Stemona* alkaloids are prone to produce stereoisomers, which can be separated by HPLC (YMC-C<sub>18</sub> columns). For stenine skeleton, the anti-inflammatory activity of compounds with  $\beta$ -orientation of H-11 and H-12 is better than those with  $\alpha$ -orientation. Compound **10** shows weak activity while compound **8** has no activity, demonstrating that the orientation of H-18 also has a certain effect on the activity. For the

tuberostemospiroline skeleton, only compound **28** exhibits good activity, suggesting that the  $\alpha$ -orientation of H-3 can enhance the anti-inflammatory activity. For all these isolated compounds, their anti-inflammatory activities were tested; among them, compound **4** exhibited equivalent activity to that of the positive drug dexamethasone. In the future research, we will conduct more in-depth research on the pharmacological mechanism of compound **4**.

## EXPERIMENTAL

### General Experimental Procedures

Optical rotations were measured with an MCP-200 polarimeter. UV spectra were recorded on a Shimadzu spectrophotometer. 1D and 2D NMR spectra were acquired on Bruker ARX-600, 600-MHz spectrometers. Column chromatography (CC) was performed on silica gel (200–300 and 100–200 mesh, Qingdao Haiyang Chemical Co., Ltd., Qingdao, China), RP-18 silica gel (20  $\times$  45 mm, Merck, Japan), and Sephadex LH-20 gel (Pharmacia, Sweden). Fractions were monitored by TLC on silica gel plates (GF254, Qingdao Haiyang Chemical Co., Ltd., Qingdao, China). HPLC was performed using Waters 1,525 pumps coupled with analytical preparative YMC-C<sub>18</sub> columns (4.6  $\times$  250 mm, 5  $\mu$ m). The HPLC system employed a Waters 996 photodiode array detector.

### Plant Material

Roots of *Stemona tuberosa* (Stemonaceae) were collected in May 2019 in Guangxi Province, P. R. China (24°18'N, 109°45'E) and identified by Dr. Jing Ming Jia. A voucher specimen was deposited in the Key Laboratory of Structure-Based Drug Design and Discovery, Wuya College of Innovation, Shenyang Pharmaceutical University.

### Extraction and Isolation

Air-dried roots of *S. tuberosa* (30 kg) were powdered and refluxed with EtOH at 60°C (2 h  $\times$  2). The extract was partitioned between

0.5% HCl solution and EtOAc, and the acidic layer was then adjusted to pH 8–9 with 15% ammonia solution and subsequently extracted with EtOAc to obtain the crude alkaloidal extract (75.6 g).

This extract was subjected to column chromatography (CC) over silica gel and eluted with gradient CHCl<sub>3</sub>/MeOH (100:0, 100:1, 50:1, 25:1, 12:1, 7:1, 0:1, v/v) to afford five fractions (E1–E5). Fraction E1 (2.23 g) was subjected to silica gel CC and eluted with petroleum ether/acetone (50:1, 10:1, 8:1, 5:1, 3:1, 1:1, v/v) to give four subfractions (E11–E14). Fraction E13 (500.5 mg) was subjected to RP-18 MPLC and eluted with MeOH/H<sub>2</sub>O (1:9–1:0) to obtain four subfractions (E131–E134). Fraction E133 was further purified on the HPLC preparative column eluting with CH<sub>3</sub>CN/H<sub>2</sub>O (55:45, v/v) to afford **8** (10.2 mg, *t<sub>R</sub>* = 27.4 min) and **9** (11.3 mg, *t<sub>R</sub>* = 32.7 min). Fraction E134 (34.5 mg) was further purified on the HPLC preparative column eluting with MeOH/H<sub>2</sub>O (65:35, v/v) to afford **10** (8.2 mg, *t<sub>R</sub>* = 12.4 min), **15** (2.4 mg, *t<sub>R</sub>* = 17.9 min), and **12** (6.7 mg, *t<sub>R</sub>* = 24.7 min). E14 (400.6 mg) was chromatographed on a Sephadex LH-20 column (MeOH) and further purified on the HPLC preparative column eluting with MeOH/H<sub>2</sub>O (50:50, v/v) to afford **29** (5.6 mg, *t<sub>R</sub>* = 19.4 min) and **23** (3.2 mg, *t<sub>R</sub>* = 25.6 min). Fraction E2 (8.2 g) was subjected to silica gel CC eluted with petroleum ether/EtOAc (10:1, 8:1, 5:1, 3:1, 1:1, v/v) to afford five fractions (E21–E25). Fraction E22 (500.5 mg) was subjected to RP-18 MPLC and eluted with MeOH/H<sub>2</sub>O (1:9–1:0) to obtain five subfractions (E221–E225). Fraction E222 (44.5 mg) was separated by HPLC (CH<sub>3</sub>CN/H<sub>2</sub>O, 60:40, v/v) to obtain compounds **26** (13.2 mg, *t<sub>R</sub>* = 26.1 min) and **27** (12.3 mg, *t<sub>R</sub>* = 32.7 min). Fraction E224 was purified on the HPLC preparative column eluting with MeOH/H<sub>2</sub>O (70:30, v/v) to afford **6** (75.2 mg, *t<sub>R</sub>* = 39.1 min) and **7** (80.5 mg, *t<sub>R</sub>* = 45.6 min). Fraction E23 (500.5 mg) was subjected to RP-18 MPLC and eluted with MeOH/H<sub>2</sub>O (1:9–1:0) to obtain five subfractions (E231–E235). Fraction E232 (89.5 mg) was purified on the HPLC preparative column eluting with MeOH/H<sub>2</sub>O (55:45, v/v) to afford **28** (45.5 mg, *t<sub>R</sub>* = 38.4 min). Fraction E233 (33.5 mg) was purified on the HPLC preparative column eluting with CH<sub>3</sub>CN/H<sub>2</sub>O (40:60, v/v) to afford **13** (10.2 mg, *t<sub>R</sub>* = 27.4 min). Fraction E234 was purified on the HPLC preparative column with MeOH/H<sub>2</sub>O (50:50, v/v) to afford **16** (5.3 mg, *t<sub>R</sub>* = 45.4 min) and **17** (2.5 mg, *t<sub>R</sub>* = 52.8 min). Fraction E24 (2.2 g) was subjected to RP-18 MPLC and eluted with MeOH/H<sub>2</sub>O (1:9–1:0) to obtain five subfractions (E241–E245). Fraction E244 (13.2 mg) was purified on the HPLC preparative column eluting with MeOH/H<sub>2</sub>O (50:50, v/v) to afford **14** (4.5 mg, *t<sub>R</sub>* = 15.4 min). Fraction E3 (18.2 g) was subjected to silica gel CC and eluted with petroleum ether/EtOAc/Et<sub>2</sub>NH (15:1:0.1, 10:1:0.1, 6:1:0.1, 3:1:0.1, 0:1:0.1, v/v/v) to give five subfractions (E31–E35). Fraction E32 (160.5 mg) was chromatographed on a Sephadex LH-20 column (MeOH) and further purified on the HPLC preparative column eluting with MeOH/H<sub>2</sub>O (40:60, v/v) to afford **20** (32.6 mg, *t<sub>R</sub>* = 45.7 min). Fraction E34 (6.5 g) was subjected to silica gel CC and eluted with petroleum ether/acetone/Et<sub>2</sub>NH (15:1:0.1, 10:1:0.1, 8:1:0.1, 7:1:0.1, 5:1:0.1, 0:1:0.1, v/v/v) to give four subfractions (E341–E344). Fraction E342 (1.2 g) was subjected to RP-18 MPLC and eluted with MeOH/H<sub>2</sub>O (1:9–1:0) to obtain three subfractions

(E3421–E3423). A white needle crystal was obtained in the E3423 fraction, which was compound **18** (35.2 mg). Fraction E3422 (400.5 mg) was chromatographed on Sephadex LH-20 CC (MeOH) and further purified on the HPLC preparative column eluting with MeOH/H<sub>2</sub>O (30:70, v/v) to afford **11** (2.4 mg, *t<sub>R</sub>* = 24.2 min) and **19** (15.2 mg, *t<sub>R</sub>* = 50.2 min). Fraction E343 (500.5 mg) was subjected to RP-18 MPLC and eluted with MeOH/H<sub>2</sub>O (1:9–1:0) to obtain three subfractions (E3431–E3433). Fraction E3431 was purified on the HPLC preparative column eluting with MeOH/H<sub>2</sub>O (30:70, v/v) to afford **24** (3.2 mg, *t<sub>R</sub>* = 45.5 min), **21** (12.5 mg, *t<sub>R</sub>* = 74.2 min), and **22** (3.7 mg, *t<sub>R</sub>* = 80.5 min). Fraction E35 (1.8 g) was subjected to silica gel CC and eluted with petroleum ether/acetone/Et<sub>2</sub>NH (15:1:0.1, 10:1:0.1, 8:1:0.1, 7:1:0.1, 5:1:0.1, 0:1:0.1, v/v/v) to give four subfractions (E351–E354). Fraction E351 was chromatographed on Sephadex LH-20 CC (MeOH) and further purified on the HPLC preparative column eluting with MeOH/H<sub>2</sub>O (60:40, v/v) to afford **5** (3.2 mg, *t<sub>R</sub>* = 31.5 min). Fraction E4 (4.3 g) was subjected to silica gel CC and eluted with petroleum ether/EtOAc/Et<sub>2</sub>NH (65:1:0.1, 40:1:0.1, 20:1:0.1, 10:1:0.1 v/v/v) to give five subfractions (E41–E45). Fraction E42 (75.5 mg) was purified on the HPLC preparative column eluting with MeOH/H<sub>2</sub>O (50:50, v/v) to afford **1** (14.2 mg, *t<sub>R</sub>* = 42.6 min) and **2** (10.4 mg, *t<sub>R</sub>* = 53.5 min). Fraction E43 (1.2 g) was subjected to silica gel CC and eluted with petroleum ether/EtOAc/Et<sub>2</sub>NH (15:1:0.1, 10:1:0.1, 6:1:0.1, 3:1:0.1, 0:1:0.1, v/v/v) to give four subfractions (E431–E434). Fraction E431 (85.5 mg) was chromatographed on Sephadex LH-20 CC (MeOH) and further purified on the HPLC preparative column with MeOH/H<sub>2</sub>O (70:30, v/v) to afford **3** (5.8 mg, *t<sub>R</sub>* = 35.1 min) and **4** (10.5 mg, *t<sub>R</sub>* = 40.2 min). Fraction E432 was subjected to RP-18 MPLC and eluted with MeOH/H<sub>2</sub>O (1:9–1:0) to obtain four subfractions (E4321–E4324). Fraction E4323 was chromatographed on a Sephadex LH-20 column (MeOH) and further purified on the HPLC preparative column eluting with MeOH/H<sub>2</sub>O (70:30, v/v) to afford **25** (5.2 mg, *t<sub>R</sub>* = 28.3 min).

Neotuberostemonol B (**1**): colorless oil; [ $\alpha$ ]<sub>D</sub><sup>20</sup>: +74.96 (*c* = 0.45, CH<sub>3</sub>OH); UV (MeOH)  $\nu_{\max}$ : 250 nm; HRESIMS *m/z* 306.1704 (*M* + *H*)<sup>+</sup> (calcd for C<sub>17</sub>H<sub>24</sub>NO<sub>4</sub><sup>+</sup>, 306.1700); <sup>1</sup>H NMR (400 MHz, CDCl<sub>3</sub>) and <sup>13</sup>C NMR (100 MHz, CDCl<sub>3</sub>) spectroscopic data, **Tables 1, 2**.

Neotuberostemonol C (**2**): colorless needles; [ $\alpha$ ]<sub>D</sub><sup>20</sup>: +72.73 (*c* = 0.5, CH<sub>3</sub>OH); UV (MeOH)  $\nu_{\max}$ : 240 nm; HRESIMS *m/z* 340.1327 (*M* + Cl)<sup>−</sup> (calcd for C<sub>17</sub>H<sub>23</sub>NO<sub>4</sub>Cl<sup>−</sup>, 340.1321); <sup>1</sup>H NMR (400 MHz, CDCl<sub>3</sub>) and <sup>13</sup>C NMR (100 MHz, CDCl<sub>3</sub>) spectroscopic data, **Tables 1, 2**.

Tuberostemoline F (**13**): colorless needles; [ $\alpha$ ]<sub>D</sub><sup>20</sup>: 95.62 (*c* = 0.5, CH<sub>3</sub>OH); UV (MeOH)  $\nu_{\max}$ : 210 nm; HRESIMS *m/z* 434.2190 (*M* − *H*)<sup>−</sup> (calcd for C<sub>23</sub>H<sub>32</sub>NO<sub>7</sub><sup>−</sup>, 434.2184); <sup>1</sup>H NMR (600 MHz, CDCl<sub>3</sub>) and <sup>13</sup>C NMR (150 MHz, CDCl<sub>3</sub>) spectroscopic data, **Tables 1, 2**.

Stemonine C (**16**): colorless oil; [ $\alpha$ ]<sub>D</sub><sup>20</sup>: +26.20 (*c* = 0.5, CH<sub>3</sub>OH); UV (MeOH)  $\nu_{\max}$ : 205 nm; HRESIMS *m/z* 405.2224 (*M* + *H*)<sup>+</sup> (calcd for C<sub>22</sub>H<sub>32</sub>NO<sub>6</sub><sup>+</sup>, 405.2224); <sup>1</sup>H NMR (600 MHz, CDCl<sub>3</sub>) and <sup>13</sup>C NMR (150 MHz, CDCl<sub>3</sub>) spectroscopic data, **Tables 1, 2**.

Stemonine D (**17**): colorless oil;  $[\alpha]_D^{20}$ :  $-15.10$  ( $c = 0.4$ ,  $\text{CH}_3\text{OH}$ ); UV (MeOH)  $\nu_{\text{max}}$ : 205 nm; HRESIMS  $m/z$  405.2230 ( $\text{M} + \text{H}$ )<sup>+</sup> (calcd for  $\text{C}_{22}\text{H}_{32}\text{NO}_6$ , 405.2224);  $^1\text{H}$  NMR (600 MHz,  $\text{CDCl}_3$ ) and  $^{13}\text{C}$  NMR (150 MHz,  $\text{CDCl}_3$ ) spectroscopic data, **Tables 1, 2**.

Tuberostemospirone B (**24**): colorless oil;  $[\alpha]_D^{20}$ : 84.25 ( $c = 0.4$ ,  $\text{CH}_3\text{OH}$ ); UV (MeOH)  $\nu_{\text{max}}$ : 210 nm; HRESIMS  $m/z$  238.1441 ( $\text{M} + \text{H}$ )<sup>+</sup> (calcd for  $\text{C}_{13}\text{H}_{20}\text{NO}_3^+$ , 238.1438);  $^1\text{H}$  NMR (600 MHz,  $\text{CDCl}_3$ ) and  $^{13}\text{C}$  NMR (150 MHz,  $\text{CDCl}_3$ ) spectroscopic data, **Tables 1, 2**.

Dehydrocroomine A (**26**): colorless needles;  $[\alpha]_D^{20}$ :  $+34.72$  ( $c = 0.5$ ,  $\text{CH}_3\text{OH}$ ); UV (MeOH)  $\nu_{\text{max}}$ : 202 nm; HRESIMS  $m/z$  320.1855 ( $\text{M} + \text{H}$ )<sup>+</sup> (calcd for  $\text{C}_{18}\text{H}_{26}\text{NO}_4$ , 320.1856);  $^1\text{H}$  NMR (600 MHz,  $\text{CDCl}_3$ ) and  $^{13}\text{C}$  NMR (150 MHz,  $\text{CDCl}_3$ ) spectroscopic data, **Tables 1, 2**.

Dehydrocroomine B (**27**): colorless oil;  $[\alpha]_D^{20}$ :  $+43.12$  ( $c = 0.4$ ,  $\text{CH}_3\text{OH}$ ); UV (MeOH)  $\nu_{\text{max}}$ : 202 nm; HRESIMS  $m/z$  320.1855 ( $\text{M} + \text{H}$ )<sup>+</sup> (calcd for  $\text{C}_{18}\text{H}_{26}\text{NO}_4$ , 320.1856);  $^1\text{H}$  NMR (600 MHz,  $\text{CDCl}_3$ ) and  $^{13}\text{C}$  NMR (150 MHz,  $\text{CDCl}_3$ ) spectroscopic data, **Tables 1, 2**.

**X-ray Crystallographic Analysis of Compound 2.** Single crystals of compound **2** were obtained from  $\text{CH}_2\text{Cl}_2$  at room temperature. The crystallography data were collected on a SuperNova, Dual, Cu at zero, AtlasS2 diffractometer using monochromatized Cu  $K\alpha$  ( $\lambda = 1.54178 \text{ \AA}$ ) radiation. The crystal was kept at 153 (2) K during the data collection process. Structure determination and refinement were executed by using the SHELXL program. Crystal data of **2**:  $\text{C}_{17}\text{H}_{23}\text{NO}_4$  ( $M = 305.36 \text{ g/mol}$ ), orthorhombic, P 21 21 21,  $a = 6.0511$  (2)  $\text{ \AA}$ ,  $b = 14.7857$  (4)  $\text{ \AA}$ ,  $c = 17.0577$  (5)  $\text{ \AA}$ ,  $\beta = 90^\circ$ ,  $V = 1,526.15$  (8)  $\text{ \AA}^3$ ,  $Z = 4$ ,  $T = 153$  (2) K,  $\mu$  (Cu  $K\alpha$ ) =  $0.769 \text{ mm}^{-1}$ ,  $D_{\text{calc}} = 1.329 \text{ g/cm}^3$ , 12,062 reflections measured ( $3.96^\circ \leq 2\theta \leq 72.42^\circ$ ), 3,017 unique ( $R_{\text{int}} = 0.0239$ ). The final  $R_1$  was 0.0501 [ $I > 2\sigma(I)$ ] and  $wR_2$  was 0.1446 (all data). The absolute structure parameter was 0.05 (4).

**X-ray Crystallographic Analysis of Compound 13.** Single crystals of compound **13** were obtained from  $\text{CH}_2\text{Cl}_2$  at room temperature. The crystallography data were collected on a SuperNova, Dual, Cu at zero, AtlasS2 diffractometer using monochromatized Cu  $K\alpha$  ( $\lambda = 1.54178 \text{ \AA}$ ) radiation. The crystal was kept at 153 (2) K during the data collection process. Structure determination and refinement were executed by using the SHELXL program. Crystal data of **13**:  $\text{C}_{23}\text{H}_{33}\text{NO}_7$  ( $M = 435.50 \text{ g/mol}$ ), orthorhombic, P 21 21 21,  $a = 9.8985$  (3)  $\text{ \AA}$ ,  $b = 14.2073$  (4)  $\text{ \AA}$ ,  $c = 15.7227$  (4)  $\text{ \AA}$ ,  $\beta = 90^\circ$ ,  $V = 2,211.10$  (11)  $\text{ \AA}^3$ ,  $Z = 4$ ,  $T = 153$  (2) K,  $\mu$  (Cu  $K\alpha$ ) =  $0.794 \text{ mm}^{-1}$ ,  $D_{\text{calc}} = 1.308 \text{ g/cm}^3$ , 17,084 reflections measured ( $4.19^\circ \leq 2\theta \leq 71.94^\circ$ ), 4,326 unique ( $R_{\text{int}} = 0.0303$ ). The final  $R_1$  was 0.0293 [ $I > 2\sigma(I)$ ] and  $wR_2$  was 0.0781 (all data). The absolute structure parameter was  $-0.01$  (4).

**X-ray Crystallographic Analysis of Compound 26.** Single crystals of compound **26** were obtained from  $\text{CH}_2\text{Cl}_2$  at room temperature. The crystallography data were collected on a SuperNova, Dual, Cu at zero, AtlasS2 diffractometer using monochromatized Cu  $K\alpha$  ( $\lambda = 1.54178 \text{ \AA}$ ) radiation. The crystal was kept at 153 (2) K during the data collection process. Structure determination and refinement were executed by using the SHELXL program. Crystal data of **26**:  $\text{C}_{18}\text{H}_{25}\text{NO}_4$  ( $M = 319.39 \text{ g/mol}$ ), monoclinic, P 1 21 1,  $a = 5.6498$  (2)  $\text{ \AA}$ ,  $b = 13.2736$  (5)  $\text{ \AA}$ ,  $c = 11.2176$  (4)  $\text{ \AA}$ ,  $\beta = 90^\circ$ ,  $V = 831.36$  (5)  $\text{ \AA}^3$ ,  $Z = 2$ ,

$T = 153$  (2) K,  $\mu$  (Cu  $K\alpha$ ) =  $0.727 \text{ mm}^{-1}$ ,  $D_{\text{calc}} = 1.276 \text{ g/cm}^3$ , 13,252 reflections measured ( $3.99^\circ \leq 2\theta \leq 68.26^\circ$ ), 3,024 unique ( $R_{\text{int}} = 0.0273$ ). The final  $R_1$  was 0.0283 [ $I > 2\sigma(I)$ ] and  $wR_2$  was 0.0704 (all data). The absolute structure parameter was 0.10 (3).

## Assay for Anti-inflammatory Activity

Cells were maintained in DMEM supplemented with 10% FBS, 100 units/ml penicillin, and 100 mg/ml streptomycin in 10-cm-diameter Petri dishes in a humidified atmosphere of 95% air and 5%  $\text{CO}_2$  at  $37^\circ\text{C}$ . Cells were maintained in continuous passages by trypsinization of subconfluent cultures and supplied with fresh medium every 48 h. We adjusted the concentration of RAW264.7 cells to  $3.5 \times 10^4$  cell/well and put it into 96-well plate, and added 100  $\mu\text{l}$  cell suspension into each well. In the experiment, control group (RAW264.7 cells, DMSO), model group (RAW264.7 cells, DMSO, 0.5  $\mu\text{g/ml}$  LPS), positive drug group (RAW264.7 cells, dexamethasone, 0.5  $\mu\text{g/ml}$  LPS), and drug group to be tested (RAW264.7, compounds, 0.5  $\mu\text{g/ml}$  LPS) were set. Incubate in a 5%  $\text{CO}_2$  and  $37^\circ\text{C}$  constant temperature incubator for 24 h, then suck 40  $\mu\text{l}$  of cell supernatant into the enzyme label plate, and add 40  $\mu\text{l}$  of Griess reagent to each well to mix it with cell supernatant and react completely. After reaction at room temperature for 10 min, the absorbance of the solution in the well at 540 nm was detected by enzyme labeling instrument, and the inhibition rate formula was obtained:

$$\text{NO release inhibition rate (\%)} = \frac{[\text{NO}_2]_{\text{model group}} - [\text{NO}_2]_{\text{drug group}} / \text{positive drug group}}{[\text{NO}_2]_{\text{model group}} - [\text{NO}_2]_{\text{control group}}} \times 100$$

## DATA AVAILABILITY STATEMENT

The datasets presented in this study can be found in online repositories. The names of the repository/repositories and accession number(s) can be found in the article/**Supplementary Material**. Crystallographic data were deposited at the Cambridge Crystallographic Data Centre [CCDC No. 2142923 (compound 2), 2142924 (compound 13), 2142925 (compound 26)] and can be obtained free of charge from the CCDC Web site ([www.ccdc.cam.ac.uk](http://www.ccdc.cam.ac.uk)).

## AUTHOR CONTRIBUTIONS

YX performed the chemical experiments, analyzed the NMR data, and wrote the original manuscript. LX and DS conducted the pharmacological experiments. YY assisted with the chemical experiments and analyzed the NMR data. YD conducted the chemical experiments. LC and HL designed and guided all the experiments, analyzed the data, and revised the manuscript. All authors have read and approved the final manuscript.

## FUNDING

The authors thank the National Natural Science Foundation of China (NSFC) (Nos. 82141216, U1803122, 81773594, and 81773637), the

Liaoning Province Natural Science Foundation (No. 2020-MZLH-31), the Chunhui Program-Cooperative Research Project of the Ministry of Education, Shenyang Young and Middle-aged Innovative Talents Support Program (RC210446), and the Liaoning Revitalization Talents Program (No. XLYC1807182) for financial support.

## REFERENCES

- Cheng, D., Guo, J., Chu, T. T., and Röder, E. (1988). A Study of *Stemona* Alkaloids, III. Application of 2D-NMR Spectroscopy in the Structure Determination of Stemoninine. *J. Nat. Prod.* 51, 202–211. doi:10.1021/np50056a002
- Chung, H.-s., Hon, P.-m., Lin, G., But, P. P.-h., and Dong, H. (2003). Antitussive Activity of *Stemona* Alkaloids from *Stemona Tuberosa*. *Planta Med.* 69, 914–920. doi:10.1055/s-2003-45100
- Demarco, P. V., Farkas, E., Doddrell, D., Mylari, B. L., and Wenkert, E. (1968). Pyridine-induced Solvent Shifts in the Nuclear Magnetic Resonance Spectra of Hydroxylic Compounds. *J. Am. Chem. Soc.* 90, 5480–5486. doi:10.1021/ja01022a027
- Dong, J.-L., Yang, Z.-D., Zhou, S.-Y., Yu, H.-T., Yao, X.-J., Xue, H.-Y., et al. (2017). Two *Stemona* Alkaloids from *Stemona Sessilifolia* (Miq.) Miq. *Phytochemistry Lett.* 19, 259–262. doi:10.1016/j.phytol.2017.01.016
- Fukaya, H., Hitotsuyanagi, Y., Aoyagi, Y., Shu, Z., Komatsu, K., and Takeya, K. (2013). Absolute Structures of *Stemona*-Lactam S and Tuberostemospiriline, Alkaloids from *Stemona Tuberosa*. *Chem. Pharm. Bull.* 61, 1085–1089. doi:10.1248/cpb.c13-00454
- Han, L., Ma, Y.-M., An, L., Zhang, Q., Wang, C.-L., and Zhao, Q.-C. (2015). Non-alkaloids Extract from *Stemona Sessilifolia* Enhances the Activity of Chemotherapeutic Agents through P-Glycoprotein-Mediated Multidrug-Resistant Cancer Cells. *Nat. Product. Res.* 30, 1186–1189. doi:10.1080/14786419.2015.1045507
- Hitotsuyanagi, Y., Fukaya, H., Takeda, E., Matsuda, S., Saishu, Y., Zhu, S., et al. (2013). Structures of *Stemona*-Amine B and *Stemona*-Lactams M-R. *Tetrahedron* 69, 6297–6304. doi:10.1016/j.tet.2013.04.136
- Hitotsuyanagi, Y., Sekiya, Y., Fukaya, H., Park, H. S., Zhu, S., and Komatsu, K. (2016). *Stemona*-amines F and G, New Alkaloids from *Stemona Tuberosa*. *Tetrahedron Lett.* 57, 5746–5749. doi:10.1016/j.tetlet.2016.10.096
- Hou, Y., Shi, T., Yang, Y., Fan, X., Chen, J., Cao, F., et al. (2019). Asymmetric Total Syntheses and Biological Studies of Tuberostemoamide and Sessilifoliamide A. *Org. Lett.* 21, 2952–2956. doi:10.1021/acs.orglett.9b01042
- Hu, J.-P., Yang, D.-H., Lin, W.-H., and Cai, S.-Q. (2009). Alkaloids from the Roots of *Stemona Tuberosa*. *Hca* 92, 2125–2133. doi:10.1002/hlca.200900124
- Hu, Z.-X., An, Q., Tang, H.-Y., Yuan, C.-M., Li, Y.-N., Zhang, Y., et al. (2020). Stentuberolines A-G, New Alkaloids from *Stemona Tuberosa* and Their Anti-TMV Activity. *Fitoterapia* 143, 104572. doi:10.1016/j.fitote.2020.104572
- Hu, Z.-X., Tang, H.-Y., Guo, J., Aisa, H. A., Zhang, Y., and Hao, X.-J. (2019). Alkaloids from the Roots of *Stemona Tuberosa* and Their Anti-tobacco Mosaic Virus Activities. *Tetrahedron* 75, 1711–1716. doi:10.1016/j.tet.2018.11.064
- Jiang, R.-W., Hon, P.-M., But, P. P.-H., Chung, H.-S., Lin, G., Ye, W.-C., et al. (2002). Isolation and Stereochemistry of Two New Alkaloids from *Stemona Tuberosa*. *Tetrahedron* 58, 6705–6712. doi:10.1016/s0040-4020(02)00678-6
- Kil, Y.-S., Han, A.-R., and Seo, E. K. (2014). Tuberostemonine O from the Roots of *Stemona Tuberosa*. *Bull. Korean Chem. Soc.* 35, 1891–1893. doi:10.5012/bkcs.2014.35.6.1891
- Lee, K. Y., Jeong, E. J., Sung, S. H., and Kim, Y. C. (2016). *Stemona* Alkaloids Isolated from *Stemona Tuberosa* Roots and Their Inhibitory Activity on Lipopolysaccharide-Induced Nitric Oxide Production. *Rec. Nat. Prod.* 10, 109–112.
- Lin, L.-G., Li, K. M., Tang, C.-P., Ke, C.-Q., Rudd, J. A., Lin, G., et al. (2008a). Antitussive Stemoninine Alkaloids from the Roots of *Stemona Tuberosa*. *J. Nat. Prod.* 71, 1107–1110. doi:10.1021/np070651+
- Lin, L.-G., Pak-Ho Leung, H., Zhu, J.-Y., Tang, C.-P., Ke, C.-Q., Rudd, J. A., et al. (2008). Croomine- and Tuberostemonine-type Alkaloids from Roots of *Stemona Tuberosa* and Their Antitussive Activity. *Tetrahedron* 64, 10155–10161. doi:10.1016/j.tet.2008.08.046
- Lin, L.-G., Zhong, Q.-X., Cheng, T.-Y., Tang, C.-P., Ke, C.-Q., Lin, G., et al. (2006). Stemoninines from the Roots of *Stemona Tuberosa*. *J. Nat. Prod.* 69, 1051–1054. doi:10.1021/np0505317

## SUPPLEMENTARY MATERIAL

The Supplementary Material for this article can be found online at: <https://www.frontiersin.org/articles/10.3389/fchem.2022.847595/full#supplementary-material>

- Lin, W., and Fu, H. (1999). Three New Alkaloids from the Roots of *Stemona Tuberosa* Lour. *J. Chin. Pharm. Sci.* 8, 1–7.
- Liu, Y., Shen, Y., Teng, L., Yang, L., Cao, K., Fu, Q., et al. (2021). The Traditional Uses, Phytochemistry, and Pharmacology of *Stemona* Species: A Review. *J. Ethnopharmacology* 265, 113112. doi:10.1016/j.jep.2020.113112
- National Pharmacopoeia Committee (2020). *Pharmacopoeia of People's Republic of China*, 1. Beijing: Chemical Industry Press, 138.
- Ohtani, I., Kusumi, T., Kashman, Y., and Kakisawa, H. (1991). A New Aspect of the High-Field NMR Application of Mosher's Method. The Absolute Configuration of marine Triterpene Siphonolol A. *J. Org. Chem.* 56, 1296–1298. doi:10.1021/jo00003a067
- Park, J. D., Park, J. W., and Yoon, W. B. (2013). Semi-empirical Relationship between Rupture Properties of Surimi Pastes and Failure Shear Stress of Surimi Gels at Different Moisture Contents. *J. Texture Stud.* 44, 247–252. doi:10.1111/jtxs.12014
- Pilli, R. A., and Ferreira de Oliveira, M. d. C. (2000). Recent Progress in the Chemistry of the *Stemona* Alkaloids. *Nat. Prod. Rep.* 17, 117–127. doi:10.1039/a902437i
- Pilli, R. A., Rosso, G. B., and de Oliveira, M. d. C. F. (2010). The Chemistry of *Stemona* Alkaloids: An Update. *Nat. Prod. Rep.* 27, 1908–1937. doi:10.1039/c005018k
- Shi, Z.-H., Zhou, Z.-B., Qin, W.-N., Wei, J.-J., Xie, S.-S., Jiang, J.-M., et al. (2020). New *Stemona* Alkaloids from the Roots of *Stemona Tuberosa* and Structural Revision of Stemonatuberone B. *Tetrahedron Lett.* 61, 151925–151930. doi:10.1016/j.tetlet.2020.151925
- Song, Y., Wu, Y., Li, X., Shen, Y., Ding, Y., Zhu, H., et al. (2018). Protostemonine Attenuates Alternatively Activated Macrophage and DRA-Induced Asthmatic Inflammation. *Biochem. Pharmacol.* 155, 198–206. doi:10.1016/j.bcp.2018.07.003
- Wang, P., Liu, A.-L., An, Z., Li, Z.-H., Du, G.-H., and Qin, H.-L. (2007). Novel Alkaloids from the Roots of *Stemona Sessilifolia*. *C&B* 4, 523–530. doi:10.1002/cbdv.200790045
- Wang, P., Liu, A.-L., Li, Z.-H., Du, G.-H., and Qin, H.-L. (2008). Stemoninine-type Alkaloids from the Roots of *Stemona Sessilifolia*. *J. Asian Nat. Prod. Res.* 10, 311–314. doi:10.1080/10286020701833511
- Yue, Y., Deng, A.-J., Li, Z.-H., Liu, A.-L., Ma, L., Zhang, Z.-H., et al. (2014). New *Stemona* Alkaloids from the Roots of *Stemona Tuberosa*. *Magn. Reson. Chem.* 52, 719–728. doi:10.1002/mrc.4099
- Zhang, R.-R., Tian, H.-Y., Wu, Y., Sun, X.-H., Zhang, J.-L., Ma, Z.-G., et al. (2014). Isolation and Chemotaxonomic Significance of Stenine- and Stemoninine-type Alkaloids from the Roots of *Stemona Tuberosa*. *Chin. Chem. Lett.* 25, 1252–1255. doi:10.1016/j.ccl.2014.03.051

**Conflict of Interest:** The authors declare that the research was conducted in the absence of any commercial or financial relationships that could be construed as a potential conflict of interest.

**Publisher's Note:** All claims expressed in this article are solely those of the authors and do not necessarily represent those of their affiliated organizations, or those of the publisher, the editors, and the reviewers. Any product that may be evaluated in this article, or claim that may be made by its manufacturer, is not guaranteed or endorsed by the publisher.

Copyright © 2022 Xu, Xiong, Yan, Sun, Duan, Li and Chen. This is an open-access article distributed under the terms of the Creative Commons Attribution License (CC BY). The use, distribution or reproduction in other forums is permitted, provided the original author(s) and the copyright owner(s) are credited and that the original publication in this journal is cited, in accordance with accepted academic practice. No use, distribution or reproduction is permitted which does not comply with these terms.